Eur Biophys J (2006) 35:675–683
DOI 10.1007/s00249-006-0076-4

ARTICLE

Changes in the level of poly(Phe) synthesis in *Escherichia coli* ribosomes containing mutants of L4 ribosomal protein from *Thermus thermophilus* can be explained by structural changes in the peptidyltransferase center: a molecular dynamics simulation analysis

G. Papadopoulos · S. Grudinin · D. L. Kalpaxis · T. Choli-Papadopoulou

Received: 20 January 2006 / Revised: 13 May 2006 / Accepted: 19 May 2006 / Published online: 14 June 2006

Abstract Data from polyphenylalanine [poly(Phe)] synthesis determination in the presence and in the absence of erythromycin have been used in conjunction with Molecular Dynamics Simulation analysis, in order to localize the functional sites affected by mutations of *Thermus thermophilus* ribosomal protein L4 incorporated in *Escherichia coli* ribosomes. We observed that alterations in ribosome capability to synthesize poly(Phe) in the absence of erythromycin were mainly correlated to shifts of A2062 and C2612 of 23S rRNA, while in the presence of erythromycin they were correlated to shifts of A2060 and U2584 of 23S rRNA. Our results suggest a means of understanding the role of the extended loop of L4 ribosomal protein in ribosomal peptidyltransferase center.

G. Papadopoulos (✉)
Department of Biochemistry and Biotechnology,
University of Thessaly, Ploutonos 26, 41221 Larissa, Greece
e-mail: papg@chem.auth.gr

S. Grudinin
Institute for Structural Biology (IBI-2),
Forschungszentrum Jülich, 52425 Jülich, Germany
e-mail: s.grudinin@fz-juelich.de

D. L. Kalpaxis
Laboratory of Biochemistry, School of Medicine,
University of Patras, 26500 Patras, Greece
e-mail: dimkal@med.upatras.gr

T. Choli-Papadopoulou
Laboratory of Biochemistry, School of Chemistry,
Aristotle University of Thessaloniki,
54006 Thessaloniki, Greece
e-mail: tcholi@chem.auth.gr

Keywords Molecular dynamics · Ribosomal function · Erythromycin

Abbreviations

Poly(Phe)	Polyphenylalanine
PTase	Peptidyltransferase
rRNA	Ribosomal RNA
TthL4	Ribosomal protein L4 from *Thermus thermophilus*
EcL22	Ribosomal protein L22 from *Escherichia coli*
MDS	Molecular dynamics simulation
wtTthL4	Wild type L4 from *Thermus thermophilus*
TthL4-Glu55	TthL4 with Gly55 replaced by Glu
TthL4-Ser55	TthL4 with Gly55 replaced by Ser
TthL4-Asp56	TthL4 with Glu56 replaced by Asp
TthL4-Gln56	TthL4 with Glu56 replaced by Gln
TthL4- Glu55Gly56	TthL4 with Gly55Glu56 inverted
RMSD	Root mean square deviation

Introduction

More than 50 different proteins in complex with rRNA compose the prokaryotic ribosome. Complete atomic structures for the large (Ban et al. 2000; Harms et al. 2001) and small (Wimberly et al. 2000; Schluenzen

et al. 2000; Brodersen et al. 2002) ribosomal subunit from bacteria were recently determined by X-ray crystallography. It is evidenced that the ribosomal primary activities, the decoding process and peptide bond formation, occur in the interior ribosomal compartment (Ban et al. 2000; Nissen et al. 2000), which is largely composed of rRNA. In the large ribosomal subunit proteins L4 and L22 protrude into the exit-tunnel region, where their extended tips along with rRNA residues form that it appears to be a gate opening (Jenni and Ban 2003). It has been suggested that the exit-tunnel, whose existence has been confirmed by crystallographic data (Nissen et al. 2000) is the normal exit path for nascent polypeptides before emerging from the ribosome (Tenson and Ehrenberg 2002). Since the exit tunnel branches at the backside of the large subunit (Gabashvili et al. 2001), additional exit possibilities may exist.

There are several speculations about the role of the exit-tunnel gate; it might function as a sensor recognizing special features of the nascent peptide chain and transmitting messages to the PTase center through L22 and L4 proteins (Nissen et al. 2000), it might provide alternative exits for the nascent peptides (Gabashvili et al. 2001; Nakatogawa and Ito 2002) or it might regulate the protein elongation cycle by stopping or modulating the traffic (Tenson and Ehrenberg 2002; Gabashvili et al. 2001). Several antibiotics inhibit protein elongation by binding to this gate (Schluenzen et al. 2001; Hansen et al. 2002; Hansen et al. 2003; Tu et al. 2005). For instance, erythromycin inhibits protein synthesis by blocking the exit-tunnel and inducing premature release of short peptidyl-tRNAs with six, seven or eight amino-acid residues (Tenson et al. 2003). Conformational distortion at the extended loop of L4 influences the catalytic properties of PTase in *Escherichia coli*, as revealed by titrating ribosomes, incorporating TthL4 mutated at positions 55 and 56, with the puromycin reaction (Leontiadou et al. 2003). In a recent work (Tsagkalia et al. 2005), several mutants of TthL4 were heterologously overproduced in *E. coli* cells. In this study, the highly conserved Glu56 in TthL4 was replaced by Asp (TthL4-Asp56) or Gln (TthL4-Gln56), while the semi-conserved Gly55 was changed to Glu (TthL4-Glu55) or Ser (TthL4-Ser55). Moreover, the sequence -Gly55Glu56- was inverted to -Glu55Gly56- (TthL4-Glu55Gly56). Incorporated into *E. coli* ribosomes, these mutants of TthL4 caused high variations in the ability of the host ribosomes to synthesize poly(Phe) and respond to erythromycin.

In the present work we used poly(Phe) synthesis data (Table 1) from this study and applied molecular dynamics simulation (MDS) analysis on models of the 50S subunit in an attempt to identify possible structural changes within the PTase center caused by the aforementioned mutations, and to relate these changes to mechanistic aspects of ribosomal function.

Materials and methods

To explain the observed changes in poly(Phe) synthetic activity and response to erythromycin of the hybrid ribosomes, possible conformational changes in the extended loop of TthL4 and ribosomal region adjacent to it were searched by MDS analysis. Thus, the region Lys52-Arg74 of wtTthL4 was modelled with Swiss-Pdb Viewer v3.7 (Guex and Peitsch 1997), using as template the loop region Arg55-Arg78 of the L4 protein from *Haloarcula marismortui*; [PDB: 1JJ2]. To imitate the natural environment of the L4 loop region that protrudes into the ribosome, the region Arg84-Ile96 of L22 from *E. coli* was also modelled using the 3D-structure of the region Gly124-Trp136 of the L22 protein from *H. marismortui* [PDB: 1JJ2]. Placement of TthL4 and EcL22 models into the rest of the *H. marismortui* 50S subunit structure [PDB: 1JJ2] was performed by energy minimization and equilibration for 100 ps at 300 K, using the Molecular Dynamics software NAMD (Kalé et al. 1999) with the CHARMM27 force field for proteins and nucleic acids. All atoms outside a sphere centred at Lys68 of TthL4 with a radius of 40 Å were fixed. This structure (wild type) served as a starting point to model all the other TthL4 mutants into the 50S subunit structure. The obtained models (including wild type) were then refined by energy minimization and equilibration for 2.1 ns at 300 K (with Langevin Thermostat), by fixing all atoms outside a sphere (radius 40 Å) centred at the midway between Lys69 of TthL4 and Lys130 of L22 (Fig. 1). About 1,490 crystallographic water molecules are included in this sphere. The electrostatic interactions inside the ribosome have been explicitly treated

Table 1 Level of poly(Phe) synthesis in the absence (–Ery) or in the presence of erythromycin (+Ery) given in Phe residues incorporated per ribosome in 60 min (Tsagkalia et al. 2005)

Assembled protein	Poly(Phe) synthesis	
	–Ery	+Ery
WtTthL4	72.9	70.3
TthL4-Glu55	33.6	6.0
TthL4-Asp56	56.1	51.3
TthL4-Ser55	96.0	19.9
TthL4-Gln56	101.3	70.8
TthL4-Glu55Gly56	128.2	72.9

via Coulomb law. All simulations were performed on the IBM p690-Cluster supercomputer in the Forschungszentrum Jülich/Germany. Our data show in most of the cases satisfying convergence as it is apparent in Fig. 1.

Results

The modeled 50S subunits were studied after energy minimization and equilibration as described in Materials and methods. The overall shape of the loop region of the TthL4 mutants did not differ significantly from that of wild type L4 (wtTthL4). This is clearly indicated in Fig. 2 which shows the loop region of TthL4 in two states, the wild type and the mutated at Gly55 and Glu56 by Glu and Gly, respectively. However, structural changes were observed in L4 structure as well as in other regions of the ribosome.

It is reasonable to assume that the level of poly(Phe) synthesis, R, primarily depends on the conformation of 50S subunit at equilibrium. For example, a change in the distance of particular atoms in the PTase center can affect directly the peptide bond formation. Such a change could be the result of a mutation at a site not belonging necessarily in the catalytic cavity. After mutating an amino acid in wtTthL4, the disturbed system adopts a conformational rearrangement. At the new equilibrium, it is presumed that the affected atoms occupy new positions and the level of poly(Phe) synthesis is changed from R_{wt} to R_m. It is also reasonable to expect that some of the atom positions are more important for the ribosome functionality than others.

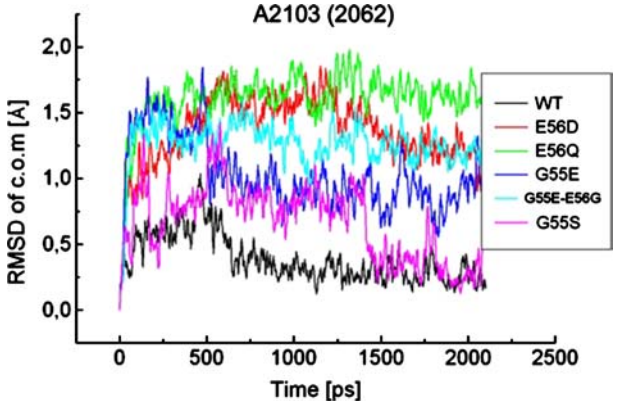

Fig. 1 Time course of RMSDs over 2.1 ns simulations for the centre of mass of residue A2103 (A2062 for *E. coli*) in 50S forms with incorporated either wild type TthL4 (*WT*) or TthL4-Asp56 (*E56D*), TthL4-Gln56 (*E56Q*), TthL4-Glu55 (*G55E*), TthL4-Glu55Gly56 (*G55E-E56G*), TthL4-Ser55 (*G55S*). The average standard deviation for the last 600 ps is 0.17 Å. The graph has been produced with Origin 4.1

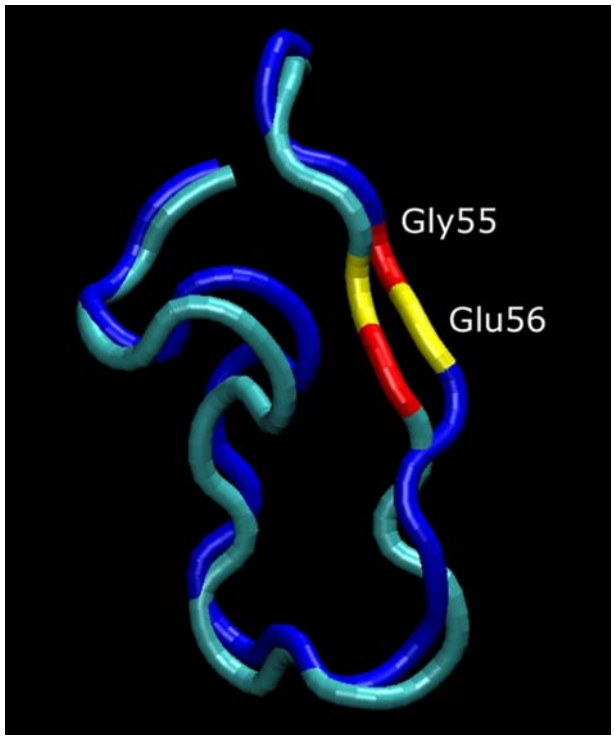

Fig. 2 Backbone representation of the extended loop region of wtTthL4 (*blue*) and TthL4-Glu55Gly56 protein (*cyan*), with numbering according to *T. thermophilus*. Gly and Glu are indicated by *red* and *yellow*, respectively. The picture has been produced with VMD (Humphrey et al. 1996)

Atoms with functional significance can be identified in a common way, via linear regression analysis between the shifts in mutant atom positions relative to their positions in the wild type on one hand and the level of poly(Phe) synthesis reached at a fixed time (60 min) on the other. Since single atoms in a molecular dynamics simulation fluctuate in a more or less stochastic way, we considered that following shifts of whole residues represented by their centre of mass, is a more safe approach. Obviously, only residues included in the defined sphere of simulation were used for this analysis. Furthermore, in order to avoid incidental results, the position of the centre of mass is calculated as an average over the last 50 ps of the simulation. The shift s_i of a residue i is defined by the relationship:

$$s_i = \sqrt{\left(x_i^m - x_i^{wt}\right)^2 + \left(y_i^m - y_i^{wt}\right)^2 + \left(z_i^m - z_i^{wt}\right)^2}, \qquad (1)$$

where x^m,y^m,z^m and x^{wt},y^{wt},z^{wt} are the coordinates of residue i in ribosomes incorporating mutant and wild type TthL4, respectively. An approximate linear relationship between the level of biosynthesis and the residue shifts relative to wild type can be derived using *transition state theory* (see Appendix) for the binding of

tRNA to the ribosome on one side, and the fact that the interaction potential between them is sensitive to displacements of groups belonging to the interface on the other. This linear approach is valid only for small but statistically significant shifts. The shifts that have been used in the present analysis meet these criteria.

The displacements of a particular residue for all five mutants define a set of shifts. Sets with at least one shift > 0.5 Å were correlated with the corresponding level of poly(Phe) synthesis in the absence (–Ery) and in the presence of erythromycin (+Ery) (Table 1). A linear regression analysis of the data was applied, in which those shifts exhibiting a correlation coefficient > 0.76 were considered as independent variables against the level of poly(Phe) synthesis. Since it was important to identify the most contributing variables to the level of poly(Phe) synthesis, we finally focused on models with two predictor variables. Thus, the equation used for the linear regression analysis was

$$y = \text{const} + a_1 s_1 + a_2 s_2, \quad (2)$$

where y represents the level of poly(Phe) synthesis and α_1 and a_2 are the regression coefficients for the independent variables s_1 and s_2, respectively. In fact, s_i are not authentic independent variables, since we can not make a mutation that separately changes only one of them, leaving the rest unaffected. Nevertheless, in the absence of any shifts, the 50S structure turns to that sustaining wtTthL4 (not valid at the mutation sites). Consequently, $R_m \rightarrow R_{wt}$ and const = R_{wt}.

Focusing on models with high correlation coefficients, we were able to identify those models that best explain our experimental data. The shift values and the regression parameters of such models are given in Tables 2 and 3, respectively. Residues 55 and 56 of TthL4 were excluded from this analysis, since the mutants contain different number of atoms. Despite the limitations and the approximate character of the above analysis, the differences found in the linear regression analysis applied in the absence and in the presence of erythromycin (different variables, different values of a_1, a_2) can be attributed to the presence or not of the drug. It is evident from Fig. 3a, that the combined shifts of A2062 and C2612 nucleosides can excellently explain the variations of poly(Phe) synthesis level in the absence of erythromycin. However, in the presence of erythromycin, it is the pair of A2060 and U2584 nucleosides which does explain the data (Fig. 3b). Although in the presence of erythromycin the G2447 and A2503 pair shows a higher correlation coefficient (Table 3), it is not very stable in respect of the signs of the regression coefficients α_1 and α_2 when regressions were performed with a higher number of independent variables and/or not a fixed const. Figures 4a and b summarize all nucleosides in the central loop of domain V of *E. coli* 23S rRNA and those amino-acid residues in TthL4 protein, whose shifts caused by the incorporation of mutant TthL4 are highly correlated to the level of poly(Phe) synthesis.

Table 2 Shifts (Å) of the mass centers, s_i, (a) of important TthL4 residues (*T. thermophilus* numbering) and (b) nucleosides in the PTase region (*H. marismortui* numbering), induced by mutations of TthL4

	TthL4 residue				
	Val57	Arg62	Pro66	His69	Gly71
(a) Assembled protein					
TthL4-Glu55	0.59	0.69	1.62	0.44	1.02
TthL4-Asp56	0.75	0.81	2.19	0.36	0.61
TthL4-Ser55	0.39	0.82	0.66	0.32	0.52
TthL4-Gln56	0.85	1.22	0.47	0.32	0.66
TthL4-Glu55Gly56	1.66	1.53	0.85	0.51	0.62

	23S rRNA nucleoside[a]							
	A2101 (A2060)	A2103 (A2062)	G2481 (G2446)	G2618 (G2583)	U2619 (U2584)	U2621 (U2586)	G2646 (C2611)	C2647 (C2612)
(b) Assembled protein								
TthL4-Glu55	0.17	0.80	1.03	0.49	0.47	0.48	0.77	1.10
TthL4-Asp56	0.33	1.22	1.48	0.50	0.43	0.45	0.67	1.22
TthL4-Ser55	0.45	0.90	0.79	0.24	0.63	0.45	0.29	0.49
TthL4-Gln56	0.68	1.37	1.25	0.80	0.40	0.54	0.40	0.88
TthL4-Glu55Gly56	0.26	2.57	2.14	0.83	0.21	0.61	0.41	1.42

[a] *E. coli* numbering is given in parenthesis

Table 3 Linear regression analysis of the most important shift-pairs (s_1, s_2) affecting the level of poly(Phe) synthesis

	Const	Residue 1	a_1	Residue 2	a_2	r
–Ery	72.9	Pro66	–45.97	G2502	168.11	0.96318
	72.9	Glu56	212.10	C2611	–148.24	0.96532
	72.9	A2062	38.54	C2611	–87.87	0.96547
	72.9	Arg62	86.61	G2505	–98.06	0.96595
	72.9	U2586	175.31	C2611	–153.35	0.96882
	72.9	Pro66	–78.96	C2064	107.07	0.97697
	72.9	G2446	137.36	C2612	–170.59	0.97995
	72.9	A2062	70.04	C2612	–84.98	0.99328
	72.9	Arg62	62.42	C2611	–104.77	0.99416
+Ery	70.3	Glu56	–388.49	Arg62	129.43	0.94324
	70.3	Gly55	–33.16	C2610	–14.23	0.94856
	70.3	His69	–349.30	G2446	82.10	0.94963
	70.3	A2060	101.45	U2584	–153.39	0.95094
	70.3	Gly71	–174.86	U2609	182.47	0.95679
	70.3	Val57	82.40	His69	–249.27	0.96272
	70.3	Gly71	–111.19	G2583	89.96	0.96358
	70.3	G2447	–180.05	A2503	186.02	0.99281

The equation used for the linear regression analysis was: $y = \text{const} + a_1 s_1 + a_2 s_2$, where const is the value of the experimental level of poly(Phe) synthesis obtained with ribosomes bearing wtTthL4, and a_1 and a_2 are the regression coefficients for the independent variables s_1 and s_2, respectively. The estimated values of the correlation coefficient r are presented in the last column. The values of s_1 and s_2 variables are given in Table 2. Nucleosides of 23S rRNA are indicated by *E. coli* numbering, while amino-acid residues of TthL4 follows *T. thermophilus* numbering

Discussion

According to crystallographic data, proteins L4 and L22 form the narrowest constriction of the nascent polypeptide chain pathway (Nissen et al. 2000). On the other hand, erythromycin binds at the entrance of the proposed exit tunnel, away from PTase center, blocking the protein synthesis by interfering with the growth of the nascent peptide chain (Schluenzen et al. 2001; Hansen et al. 2002; Zengel et al. 2003). As demonstrated previously (Tsagkalia et al. 2005), ribosomes containing the endogenous EcL4 or wtTthL4 are insensitive against erythromycin and the effects of some mutations can be partially explained by the relatively lower content of these ribosomal populations in 70S particles (the functional unit) and the moderate efficiency for tRNA binding to their A-site.

According to our MDS analysis and the subsequent treatment of the data by linear regression analysis, the changes in poly(Phe) synthesis in the absence of erythromycin can be attributed predominantly to shifts of nucleosides A2062, G2446, G2502, G2505, U2586, C2611, and C2612 in 23S rRNA (*E. coli* numbering) as well as to displacements of Arg62 and Pro66 in TthL4 mutants from their positions in the wild-type structure. These effects may be mediated through alterations in the local conformation of the region close to the entrance of the exit-tunnel. However, since the efficiency of the mutated ribosomes was found to be related with their A-site binding capability (Tsagkalia et al. 2005), it seems more likely that the conformation of A-site may be targeted by remote modifications that are conveyed through TthL4 backbone and 23S rRNA over a distance of 35–38 Å. Among the variables, the combinations of A2062 with C2612 shifts and Arg62 with C2611 shifts exhibit the highest correlation coefficient values against the level of poly(Phe) synthesis. In both cases, the C2611 and C2612 shifts contribute negatively ($\alpha_2 < 0$), while the A2062 shifts affect positively the level of poly(Phe) synthesis. Nucleosides C2611 and C2612 are involved in base-pairing interactions with nucleosides G2057 and G2056, respectively (Fig. 4a). Previous mutational studies have indicated that disruption of those base-pairs leads to significant growth disadvantages and low susceptibility of ribosomes to 14-membered macrolides (Vester and Douthwaite 2001). Surprisingly, even an alteration of the A2057•U2611 base-pair to G•C confers substantial decrease to the growth rate of an A2058G mutant of *Mycobacterium smegmatis* (Pfister et al. 2005), a fact emphasizing the strategic role of this base-pair in the local conformation of ribosomes. These observations may explain the negative character of C2611- and C2612-shift contribution to the level of poly(Phe) synthesis. On the other hand, A2062 is midway between the A-site crevice and the entrance of the exit-tunnel (Hansen et al. 2003). Therefore, it can interact with tRNAs and antibiotics bound at either region. In addition, the conformation of A2062 is very flexible and depends on whether ligands are/or are not bound

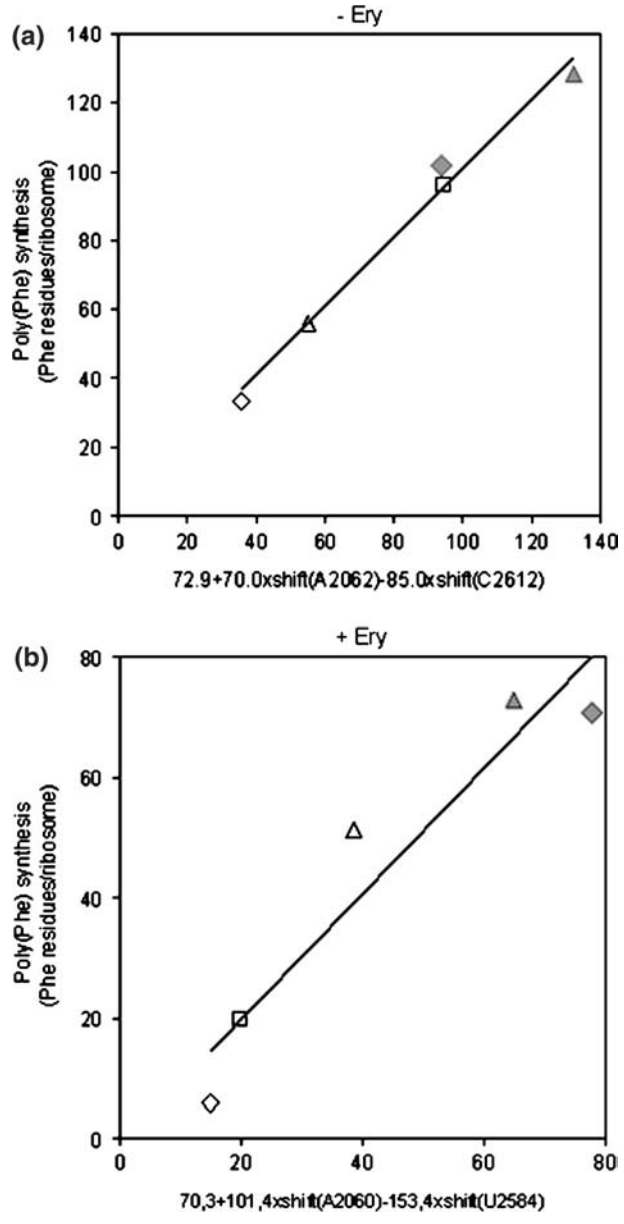

Fig. 3 Correlation of the poly(Phe) synthesis level with the linear function of 23S rRNA residue shifts (displacements of mass centers) induced by mutations in the extended loop of TthL4. Poly(Phe) synthesis was carried out **a** in the absence or **b** in the presence of erythromycin. The values of shifts shown in the function of horizontal axis were taken from Table 2, and correspond to (*open diamond*) TthL4-Glu55, (*open triangle*) TthL4-Asp56, (*open square*) TthL4-Ser55, (*filled diamond*) TthL4-Gln56, and (*filled triangle*) TthL4-Glu55Gly56 mutants. The linear regression parameters are shown in Table 3

to the ribosome (Nissen et al. 2000; Hansen et al. 2003). This fact supports the suggestion that the identified A2062 shifts may facilitate the correct positioning of Phe-tRNA^{Phe} at the A-site, thereby positively affecting the protein-synthesizing machine. A model of the structural changes in the region close to A2062 in 23S rRNA (A2103 in *H. marismortui*), induced by the incorporated TthL4-Glu55Gly56 protein, is given in Fig. 5a. With regards to other nucleosides whose shifts affect poly(Phe) synthesis, it has been previously demonstrated that they influence the growth phenotype, by affecting the substrate binding to the A-site or the translocation process. For instance, G2446 is placed adjacently to the phylogenetically conserved base-pair C2063•G2447, whose opening confers slow growth and erythromycin-sensitive phenotype (Douthwaite and Aagaard 1993). Also, G2505 is protected by puromycin and erythromycin against kethoxal (Rodriguez-Fonseca et al. 2000; Moazed and Noller 1987), while the neighbor nucleoside U2506 is around 9 Å from the position of A2451, a footprint of the A-site (Yusupov et al. 2001). Both G2505 and U2506 cross-link to photoreactive aminoacyl-tRNA analogs bound at the A- or P-sites (Steiner et al. 1988).

The level of poly(Phe) synthesis in the presence of erythromycin is mainly related to conformational rearrangements of nucleosides A2060 and U2584. Shifts of U2584 increase the sensitivity of the mutant ribosomes to erythromycin (Table 3). This is probably mediated by destabilization of the P-site substrate. Our hypothesis is supported by the suggestion that U2585 placed next to U2584, anchors the rotatory motion of the tRNA-3′ end from the A- to the P-site and assures the proper positioning of P-site substrates (Agmon et al. 2004). Since erythromycin destabilizes this interaction and causes drop-off of peptidyl-tRNAs (Lovmar et al. 2004), it is likely that U2584 shifts facilitate the destabilization effect of erythromycin and, therefore, confers a low ribosomal catalytic activity. Shifts of A2059 and A2060 cause the opposite effect. The first nucleoside belongs to the binding pocket of erythromycin in wild-type *E. coli* and susceptible *H. marismortui* large ribosomal subunits as shown by crystallographic studies (Schluenzen et al. 2001; Tu et al. 2005). Therefore, it is reasonable to suppose that shifts of these nucleosides may directly affect the susceptibility of ribosomes to the drug. A model of the structural changes in the region close to A2060 (A2101 in *H. marismortui*) induced by the incorporated TthL4-Glu55Gly56 protein, is given in Fig. 5b. Other nucleosides, whose shifts compensate for the loss of ribosomal activity in the presence of erythromycin, are G2446, m^{2}A2503 and U2609. As shown (Tu et al. 2005), A2538 in *H. marismortui* ribosomes (m^{2}A2503 in *E. coli*) participates in the pocket that fits the hydrophobic face of erythromycin with the tunnel wall. In addition, in the crystallographic structure provided by Schluenzen et al. (2000) the O4 of U2609 is within hydrogen-bonding

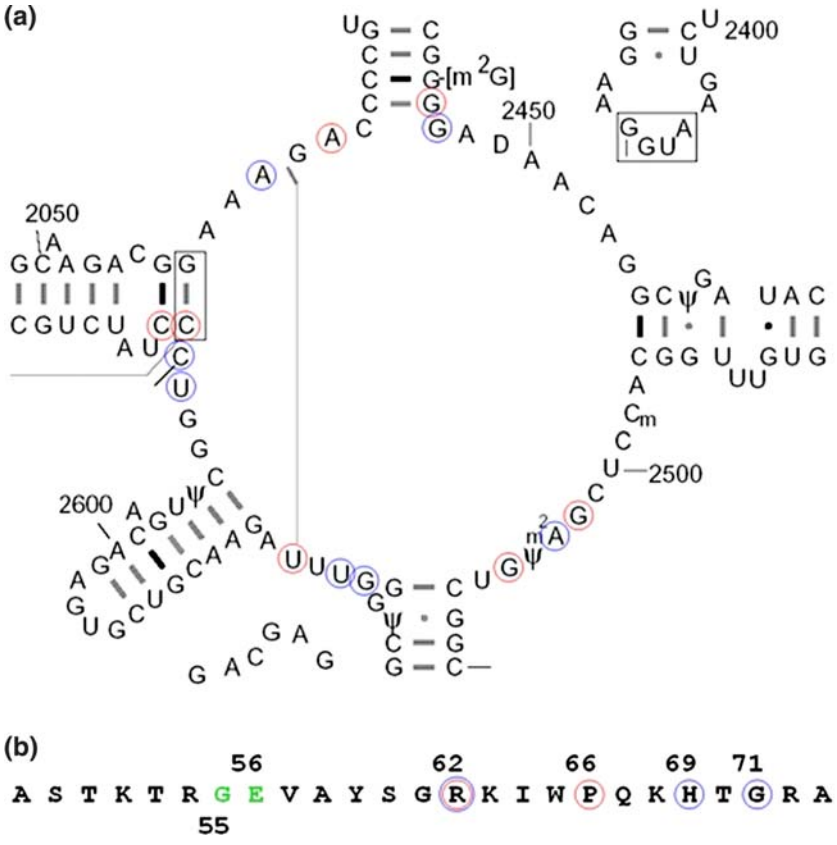

Fig. 4 **a** Secondary structure map of the central loop of domain V of *E. coli* 23S rRNA; residues marked *red* indicate nucleosides whose shifts are highly correlated to the level of poly(Phe) synthesis carried out in the absence of erythromycin, while residues marked *blue* indicate nucleosides whose shifts are correlated to the level of poly(Phe) performed in the presence of the drug. **b** Sequence of the extended loop region of TthL4 (*T. thermophilus* numbering). Amino acids whose shifts are correlated to the level of poly(Phe) synthesis, are marked as outlined in (**a**). The mutated amino acids in TthL4 are shown in *green*

distance to the 11-OH group of the lactone ring. Therefore, changes in the position of U2609 would be expected to perturb the conformation of erythromycin binding pocket. In contrast, shifts of Glu56, Gly55, His69, Gly71 and His69 in TthL4 species (*T. thermophilus* numbering) cause enhancement of ribosome susceptibility to the drug. A direct effect of the latter shifts on erythromycin structure cannot be easily speculated; structural studies have denied any direct interaction of L4 with erythromycin (Schluenzen et al. 2001). Therefore, certain mutations in TthL4 species are again presumed to induce a re-organization of the erythromycin-binding region through a remote effect.

Our results provide support to the proposed hypothesis that the exit-tunnel gate might function as a sensor recognizing special features of the nascent peptide chain or ligands, like antibiotics, and transmitting messages to the PTase centre through ribosomal proteins and 23S rRNA. The above conclusions are based on MDS analysis, which must be considered with caution. Both the approximate modeling of 50S subunit and the limitations set may lead to unreasonable interpretations, if one does not view the present results as a way to localize functional regions disturbed by non-local effects.

Appendix

In this section, a justification is given for the application of a linear regression analysis to identify distant groups affected by the mutations. First, we start with a simplification of the complex process of the protein elongation step, by assuming that the binding of the aminoacyl-tRNA to the A-site pocket is the rate limiting step. According to the transition state theory,

$$\text{Kinetic scheme 1}: \mathrm{L} + \mathrm{S} \rightleftarrows (\mathrm{LS})^{\neq} \rightarrow \mathrm{LS}$$

where L is the ligand (aminoacyl-tRNA), S is the acceptor molecule (mRNA-programmed ribosome, containing peptidyl-tRNA at the P-site), and LS is the encounter complex prior to peptide bond formation.

The rate constant k of the overall reaction is given by

$$k = \frac{k_{\mathrm{B}} T}{h} \mathrm{e}^{-\Delta G^{\neq}/RT}, \tag{3}$$

where $\Delta G^{\neq} = G^{\neq}_{\mathrm{LS}} - (G_{\mathrm{L}} + G_{\mathrm{S}})$.

In the latter relationship, $\Delta G^{\neq}$ is the activation energy, $G^{\neq}_{\mathrm{LS}}$ is the free energy of the activated complex, and G_{L}, G_{S} are the free energies of the ligand and the acceptor molecule, respectively. The symbols T, k_{B}

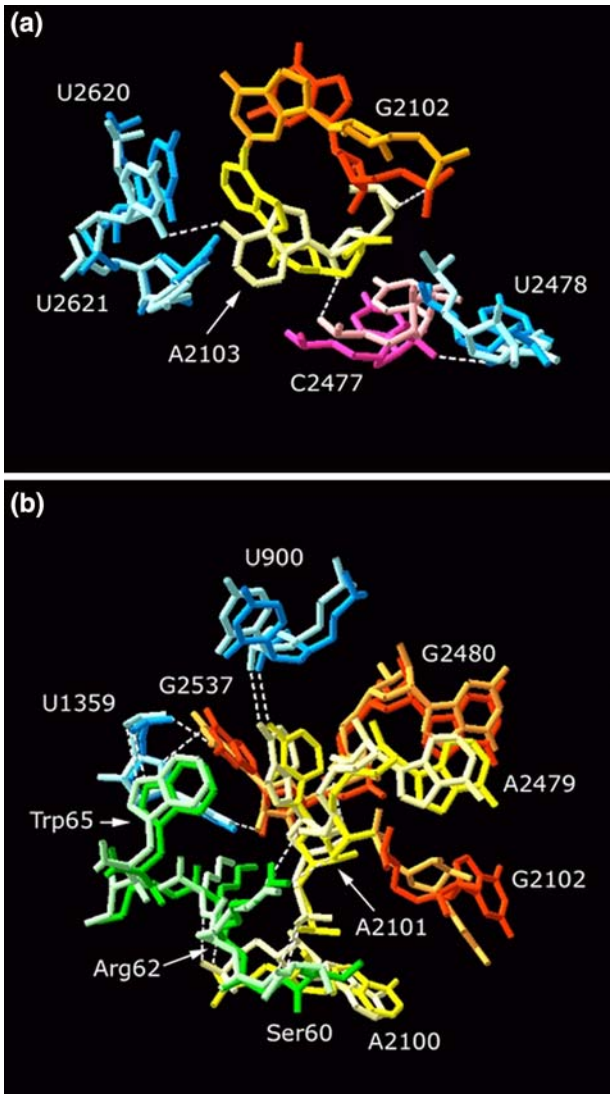

Fig. 5 Three-dimensional representation showing structural changes induced by the TthL4-Glu55Gly56 mutant in the region close **a** to A2103 or **b** to A2101 nucleosides (*H. marismortui* numbering). Nucleosides are colored according to their base (A, *yellow*; C, *pink*; G, *orange*; U, *blue*). Wild type conformations are distinguished by lighter colors. The pictures have been generated by using the Swiss-PdbViewer v3.7 (Guex and Peitsch 1997)

and h have their usual meaning. It might be expected that the activation energy depends on the conformation of the binding pocket and that of the ligand (aminoacyl-tRNA). Also, it might be expected that some conformations of the binding pocket favor binding (smaller $\Delta G^{\neq}$) while others prevent it (higher $\Delta G^{\neq}$). It is reasonable to assume that the major contribution to the dependence of $\Delta G^{\neq}$ on conformational changes comes from $G_{\mathrm{LS}}^{\neq}$. This is because aminoacyl-tRNA is not disturbed by the mutations and because the changes of G_{S} are small compared with changes of the interaction energy between n groups at the $(LS)^{\neq}$ interface. Lets denote by δ_i the distance of an individual residue i of S at the interface with L from its counterpart at L. The interaction potential between these individual groups is assumed to be of the Lennard-Jones type. For small changes in δ_i, leaving the system on the same side of the potential well, we can roughly adopt a linear dependence of the interaction potential on δ_i. Other factors contributing to the activation energy do not significantly depend on δ_i and therefore,

$$\frac{\partial \Delta G^{\neq}}{\partial \delta_i} \sim \left\langle \frac{\partial U}{\partial \delta_i} \right\rangle \sim \gamma_i. \tag{4}$$

In Eq. 4, U is the total interaction potential of all trans-interacting groups at the interface, and γ_i are constants. The symbols "~" and " $\langle\rangle$" denote proportionality and ensemble averaging correspondingly.

After mutating an amino acid at the extended loop of L4, the disturbed system adopts a new equilibrium for residue positions (near the original), leading to a change $\mathrm{d}\delta_i$ in δ_i. In turns, this leads to a change in the rate constant,

$$\mathrm{d}k = -k\frac{\partial \Delta G^{\neq}}{RT\partial \delta_1}\mathrm{d}\delta_1 - k\frac{\partial \Delta G^{\neq}}{RT\partial \delta_2}\mathrm{d}\delta_2 - \cdots - k\frac{\partial \Delta G^{\neq}}{RT\partial \delta_n}\mathrm{d}\delta_n. \tag{5}$$

Equation 5 combines with 4 to give the relationship

$$\mathrm{d}k = \sum_{i=1}^{n} \beta_i \mathrm{d}\delta_i, \tag{6}$$

where $\beta_i \approx -\frac{k_{\mathrm{wt}}\gamma_i}{RT}$, and k_{wt} is the rate constant for the wild type.

We can use similar considerations to generalize the above analysis to include all N interacting groups in the ribosome and express the overall change of the experimentally measured level of poly(Phe) synthesis in 60 min, R, as a linear function of $\mathrm{d}\delta_i$. We use as a measure of $\mathrm{d}\delta_i$ what we call here shifts, s_i, given by the relationship

$$s_i = \sqrt{(x_i^{\mathrm{m}} - x_i^{\mathrm{wt}})^2 + (y_i^{\mathrm{m}} - y_i^{\mathrm{wt}})^2 + (z_i^{\mathrm{m}} - z_i^{\mathrm{wt}})^2}, \tag{7}$$

where x^{m},y^{m},z^{m} and x^{wt},y^{wt},z^{wt} are the equilibrium coordinates of the residues' mass centres. Hence:

$$\mathrm{d}R = \sum_{i=1}^{N} \alpha_i s_i \text{ or } R_m = R_{wt} + \sum_{i=1}^{N} \alpha_i s_i. \tag{8}$$

Coefficients α_i summarize all parameters affecting R, which do not depend on mutations.

Concerning the sum in Eq. 8, we notice that most of its terms contribute very little because of relatively small s_i or/and small α_i. Moreover, since α_i can be positive or negative, they can cancel each other in many cases. On the other hand there must be some regions of the 50S subunit, like the PTase center, that are expected to contribute largely. In the frame of this analysis, we tried to identify the residues that exhibit the largest contributions in the sum of Eq. 8, keeping only two variables in the regression analysis. Of course this is not a rigorous analysis. Nevertheless, it is operationally a useful one, since a posteriori the results of the regression analysis are meaningful.

References

Agmon I, Amit M, Auerbach T, Bashan A, Baram D, Bartels H, Berisio R, Greenberg J, Harms J, Hansen HAS, Kessler M, Pyetan E, Schluenzen F, Sittner A, Yonath A, Zarivach R (2004) Ribosomal crystallography: aflexible nucleotide anchoring tRNA translocation, facilitates peptide-bond formation, chirality discrimination and antibiotics synergism. FEBS Lett 567:20–26

Ban N, Nissen P, Hansen J, Moore PB, Steitz TA (2000) The complete atomic structure of the large ribosomal subunit at 2.4 Å resolution. Science 289:905–920

Brodersen DE, Clemons Jr WM, Carter AP, Wimberly BT, Ramakrishnan V (2002) Crystal structure of the 30S ribosomal subunit from *Thermus thermophilus*: structure of the proteins and their interactions with 16S RNA. J Mol Biol 316:725–768

Douthwaite S, Aagaard C (1993) Erythromycin binding is reduced in ribosomes with conformational alterations in the 23S rRNA peptidyl transferase loop. J Mol Biol 232:725–731

Gabashvili IS, Gregory ST, Valle M, Grassucci R, Worbs M, Wahl MC, Dahlberg AE, Frank J (2001) The polypeptide tunnel system in the ribosome and its gating in erythromycin resistance mutants of L4 and L22. Mol Cell 8:181–188

Guex N, Peitsch MC (1997) SWISS-MODEL and the Swiss-PdbViewer: an environment for comparative protein modelling. Electrophoresis 18:2714–2723

Hansen JL, Ippolito JA, Ban N, Nissen P, Moore PB, Steitz TA (2002) The structure of four macrolide antibiotics bound to the large ribosomal subunit. Mol Cell 10:117–128

Hansen JL, Moore PB, Steitz TA (2003) Structures of five antibiotics bound at the peptidyl transferase center of the large ribosomal subunit. J Mol Biol 330:1061–1075

Harms J, Schluenzen F, Zarivach R, Bashan A, Gat S, Agmon I, Bartels H, Franceschi F, Yonath A (2001) High resolution structure of the large ribosomal subunit from a mesophilic eubacterium. Cell 107:679–688

Humphrey W, Dalke A, Schulten K: VMD (1996) Visual molecular dynamics. J Mol Graph 14:33–38

Jenni S, Ban N (2003) The chemistry of protein synthesis and voyage through the ribosomal tunnel. Curr Opin Struct Biol 13:212–219

Kalé L, Skeel R, Bhandarkar M, Brunner R, Gursoy A, Krawetz N, Phillips J, Shinozaki A, Varadarajan K, Schulten K (1999) NAMD2: greater scalability for parallel molecular dynamics. J Comput Phys 151:283–312

Leontiadou F, Xaplanteri MA, Papadopoulos G, Gerassimou C, Kalpaxis DL, Choli-Papadopoulou T (2003) On the structural and functional importance of the highly conserved Glu56 of *Thermus thermophilus* L4 ribosomal protein. J Mol Biol 332:73–84

Lovmar M, Tenson T, Ehrenberg M (2004) Kinetics of macrolide action: the josamycin and erythromycin cases. J Biol Chem 279:53506–53515

Moazed D, Noller HF (1987) Chloramphenicol, erythromycin, carbomycin and vernamycin B protect overlapping sites in peptidyl transferase region of 23S ribosomal RNA. Biochimie 69:879–884

Nakatogawa H, Ito K (2002) The ribosomal exit tunnel functions as discriminating gate. Cell 108:629–636

Nissen P, Hansen J, Ban N, Moore PB, Steitz TA (2000) The structural basis of ribosome activity in peptide bond synthesis. Science 289:920–930

Pfister P, Corti N, Hobbie S, Bruell C, Zarivach R, Yonath A, Böttger EC (2005) 23S rRNA base pair 2057–2611 determines ketolide susceptibility and fitness cost of the macrolide resistance mutation 2058A → G. Proc Natl Acad Sci USA 102:5180–5185

Rodriguez-Fonseca C, Phan H, Long KS, Porse BT, Kirillov SV, Amils R, Garrett RA (2000) Puromycin-rRNA interaction sites at the peptidyl transferase center. RNA 6:744–754

Schluenzen F, Tocilj A, Zarivach R, Harms R, Harms J, Gluehmann M, Janell D, Bashan A, Bartels H, Agmon I, Franceschi F, Yonath A (2000) Structure of functionally activated small ribosomal subunit at 3.3 angstroms resolution. Cell 102:615–623

Schluenzen F, Zarivach R, Harms J, Bashan A, Tocilj A, Albrecht A, Yonath A, Franceschi F (2001) Structural basis for the interaction of antibiotics with the peptidyl transferase center in eubacteria. Nature 413:814–821

Steiner G, Kuechler E, Barta A (1988) Photo-affinity labeling at the peptidyl transferase center reveals two different positions for the A- and P-sites in domain V of 23S rRNA. EMBO J 7:3949–3955

Tenson T, Ehrenberg M (2002) Regulatory nascent peptides in the ribosomal tunnel. Cell 108:591–594

Tenson T, Lovmar M, Ehrenberg M (2003) The mechanism of action of macrolides, lincosamides and streptogramin B reveals the nascent peptide exit path in the ribosome. J Mol Biol 330:1005–1014

Tsagkalia A, Leontiadou F, Xaplanteri MA, Papadopoulos G, Kalpaxis DL, Choli-Papadopoulou T (2005) Ribosomes containing mutants of L4 ribosomal protein from *Thermus thermophilus* display multiple defects in ribosomal functions and sensitivity against erythromycin. RNA 11:1633–1639

Tu D, Blaha G, Moore PB, Steitz TA (2005) Structures of MLS_BK antibiotics bond to mutated large ribosomal subunits provide a structural explanation for resistance. Cell 121:257–270

Vester B, Douthwaite S (2001) Macrolide resistance conferred by base substitutions in 23S rRNA. Antimicrob Agents Chemother 45:1–12

Wimberly BT, Brodersen DE, Clemons WM Jr, Morgan-Warren RJ, Carter AP, Vonrhein C, Hartsch T, Ramakrishnan V (2000) Structure of the 30S ribosomal subunit. Nature 407:327–339

Yusupov MM, Yusupova GZ, Baucom A, Lieberman K, Earnest TN, Cate JHD, Noller HF (2001) Crystal structure of the ribosome at 5.5 Å resolution. Science 292:883–896

Zengel JM, Jerauld A, Walker A, Wahl MC, Lindahl L (2003) The extended loops of ribosomal proteins L4 and L22 are not required for ribosomal assembly or L4-mediated autogenous control. RNA 9:1188–1197